The Influence of End Frictions on Stresses in Compressed Specimens

AUTHOR(S):

NIWA, Yoshiji; KOBAYASHI, Shoichi; NAKAGAWA, Koji

CITATION:

NIWA, Yoshiji ...[et al]. The Influence of End Frictions on Stresses in Compressed Specimens. Memoirs of the Faculty of Engineering, Kyoto University 1969, 31(1): 1-11

ISSUE DATE:

1969-03-25

URL:

http://hdl.handle.net/2433/280759

The Influence of End Frictions on Stresses in Compressed Specimens

By

Yoshiji NIWA*, Shoichi KOBAYASHI* and Koji NAKAGAWA*

(Received September 30, 1968)

The present paper concerns the influences of end frictions on stresses in compressed rectangular and cylindrical specimens. In numerical caluculations, the finite element method was employed. The following conclusions are made on the influences of the end frictions on stresses in the compressed specimens.

(i) The more the end friction between the end of the specimen and the platten is reduced the more uniform stresses are developed in the specimen.

(ii) When Poissoin's ratio is 1/6 and the coefficients of the end friction are approximately larger than 0.25, no lubrication can be practically expected, in other terms stresses in specimens with such coefficients of end friction are practically the same as stresses in specimens completely restrained at the ends.

(iii) Stresses in both rectangular and cylindrical specimens are similar. The only difference is that the deviations of the axial stresses for various coefficients of frictions from the average are larger in cylindrical specimens than those in rectangular ones.

(iv) Stresses in the mid-height region of the specimens are not so sensitive to the end friction as the compressed ends. Uniformity of stresses depends on the width-height or radius-height ratios as well as the end frictions.

(v) For sufficiently small coefficients of the end friction, some portions of the end of the specimen slide and the shear stresses on the end become terrace-like and axial stressses become more or less uniform.

1. Introduction

It is of fundamental importance to analyse stresses in compressed specimens in order to study the strength and the mechanism of failure of brittle materials.

The compressive strength of brittle materials is conventionally expressed by an average stress which is given by the axial load at failure divided by the sectional area of the specimen, even when stresses are not completely uniaxial. In the so-called uniaxial compression test, stresses are usually not uniform throughout the specimen, because the ends of the specimen are restrained by the work of frictions developed between the ends of the specimen and the plattens. The less the

* Department of Civil Engineering.

friction becomes, the more uniform stresses may be developed in the specimen.

In the limit case that no friction works, stresses become uniform throughout the specimen.

In what follows, we shall discuss the influence of the end frictions on the stresses in compressed specimens, which are obtained approximately by the use of the finite element method.

2. Presentation of Problems

Two types of problem will be considered in the following.

(I) Rectangular block specimens in the state of plane strain. We consider a rectangular block specimen compressed between two parallel rigid plattens as shown in Fig. 1 with the rectangular Cartesian coordinate system. The specimen is assumed in the state of plane strain.

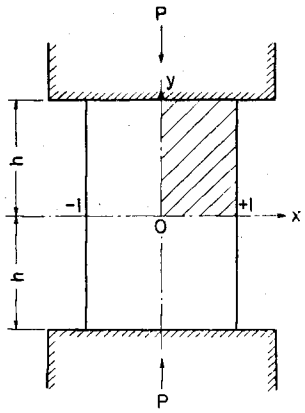

Fig. 1. Rectangular specimen and rectangular coordinates.

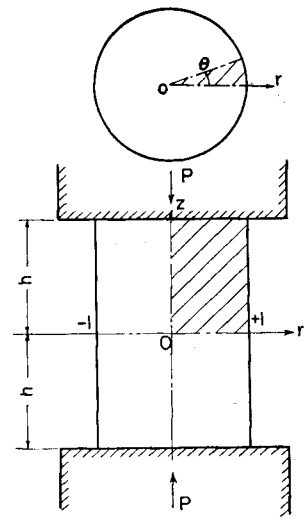

Fig. 2. Cylindrical specimen and cylindrical coordinates.

(II) Cylindrical specimens. We consider a cylindrical specimen compressed axially between two parallel rigid plattens. Cylindrical coordinates are taken as shwon in Fig. 2.

In both cases, the specimens are assumed to behave elastically and the apparent coefficients of friction developed between the ends of the specimens and the plattens are assumed to remain constant along the interface of the specimens and the plattens without regard to the magnitude of stresses. When the specimens are compressed in y(or z)-direction, they expand in x(or r)-direction. The ends of the

specimen, however, restrained by the plattens through the action of the friction and the specimen becomes bulged. The less restrained the specimen is, the less bulged it becomes and the more uniform stresses develope. When the coefficient of friction μ is sufficiently small, some portions of the compressed ends of the specimen slide outwards, when such a condition is fulfilled that the ratio of the tangential stress τ_{xy}(or τ_{rz}) to the normal stress σ_y(or σ_z) becomes equal to the coefficient of friction μ.

Along the interface of the specimen and the platten the following conditions must be satisfied:

for (I) the rectangular specimen,

$$\begin{aligned} |\tau_{xy}(x, \pm h)| &< -\sigma_y(x, \pm h)\mu \quad \text{for fixed portions,} \\ &= -\sigma_y(x, \pm h)\mu \quad \text{for slided portions} \end{aligned} \tag{2-1}$$

and for (II) the cylindrical specimen,

$$\begin{aligned} |\tau_{rz}(r, \pm h)| &< -\sigma_z(r, \pm h)\mu \quad \text{for fixed portions,} \\ &= -\sigma_z(r, \pm h)\mu \quad \text{for slided portions.} \end{aligned} \tag{2-2}$$

3. Numerical Procedures

The finite element method may be advantageously applied to this type of problem, though it is an approximate method. In the finite element method, the external forces $\{\boldsymbol{R}\}$ and the corresponding nodal displacements $\{\boldsymbol{\delta}\}$ are related by the following equation

$$\{\boldsymbol{R}\} = [\boldsymbol{K}]\{\boldsymbol{\delta}\} \tag{3-1}$$

when matrix $[\boldsymbol{K}]$ represents

$$K_{ij} = \Sigma\, k_{ij} \tag{3-2}$$

and k_{ij} is the stiffness matrix of individual specimen elements. The stiffness matrix of an element is represented by

$$[\boldsymbol{k}]^e = \int [\boldsymbol{B}]^{\mathrm{T}}[\boldsymbol{D}][\boldsymbol{B}]\, t\, dx\, dy \tag{3-3}$$

in two dimensional case, and

$$[\boldsymbol{k}]^e = \int [\boldsymbol{B}]^{\mathrm{T}}[\boldsymbol{D}][\boldsymbol{B}]\, r\theta\, dr\, dz \tag{3-4}$$

in axi-symmetric case, where t is the thickness of the element. $[\boldsymbol{D}]$ and $[\boldsymbol{B}]$ matrices are different in both cases. In integrating the above equations, it is assumed that $[\boldsymbol{B}]$, $[\boldsymbol{D}]$ and t are constant in an element, and we obtain

$$[\boldsymbol{k}]^e = [\boldsymbol{B}]^{\mathrm{T}}[\boldsymbol{D}][\boldsymbol{B}]t\Delta \tag{3-5}$$

in two dimensional problem.

In axi-symmetric problem, $[\boldsymbol{B}]$ is a function of r and z, the integration is not so simple. As the most simple assumption, we assume that r and z are constants as expressed by $\bar{r}$ and $\bar{z}$

$$\begin{aligned} \bar{r} &= (r_i+r_j+r_k)/3 \\ \bar{z} &= (z_i+z_j+z_k)/3 \end{aligned} \tag{3-6}$$

as shown in Fig. 3, then Eq. (3-4) becomes

$$[k]^e = [\bar{B}]^{\mathrm{T}}[D][\bar{B}]\bar{r}\theta\Delta \tag{3-7}$$

where Δ represents the area of the triangular element.

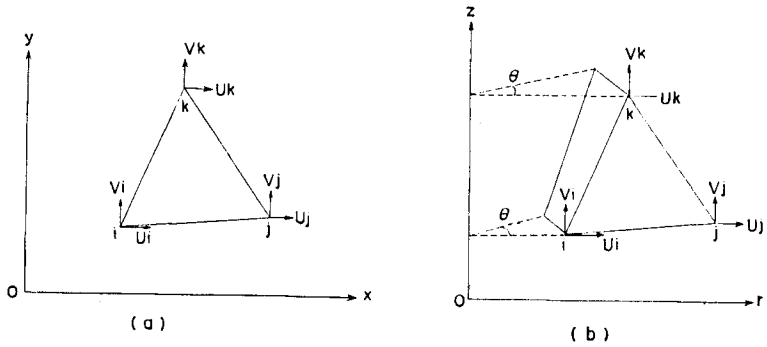

Fig. 3. Triangular elements (a) Two-dimensional case, (b) Axi-symmetric case.

In the finite element method, given external forces are represented by nodal forces. When boundary conditions are given in stresses, surface tractions must be replaced by the nodal forces which are equivalent in effect to the surface tractions (in the sense of St. Venant).

Let us take the nodal points I-1, I, I+1 on x-axis with x-coordinates l, m, n, respectively. The nodal force acting at the node I is given by

$$P(I) = t\int_{(l+m)/2}^{(m+n)/2} p(x)\,dx \tag{3-8}$$

$$P(I) = t\int_{I}^{m}\left(\frac{x-l}{m-l}\right)p(x)dx + t\int_{m}^{n}\left(\frac{x-n}{m-n}\right)p(x)dx \tag{3-9}$$

Conversely, when we must resolve the calculated nodal forces into the distributed loads on the boundary (such a case occurs when boundary displacements are given), we may assume the linear distribution of the loads in the integration interval. With

this assumption the distributed load in the two dimensional case is given by

$$p(m) = \frac{2}{t(n-l)} P(I) \tag{3-10}$$

and is identical in both methods.

In axi-symmetric problem, it is advisable to remember that the nodal forces act on the co-central arcs. Here two simple cases are considered. The first is

$$P(I) = \int_0^\theta d\theta \int_{(I+m)/2}^{(m+n)/2} p(r) r dr \tag{3-11}$$

and the second is

$$P(I) = \int_0^\theta d\theta \int_I^m \left(\frac{r-l}{m-l}\right) p(r) r\, dr + \int_0^\theta d\theta \int_m^n \left(\frac{r-n}{m-n}\right) p(r) r dr \tag{3-12}$$

With the assumption of linear distribution of the external loads with respect to r in the integration interval, we have

$$p(s) = \frac{P(I)}{\int_0^\theta d\theta \int_{(m+I)/2}^{(m+n)/2} r dr} \tag{3-13}$$

and

$$p(s) = \frac{P(I)}{\int_0^\theta d\theta \int_I^m \left(\frac{r-l}{m-l}\right) dr + \int_0^\theta d\theta \int_m^n \left(\frac{r-n}{m-n}\right) r dr} \tag{3-14}$$

Stresses on the boundary may be derived in the same manner, that is, the normal component and the tangential component of the individual nodal force are resolved into the normal and the tangential surface tractions, which are equal to the normal and tangential stresses on the boundary, respectively.

In the actual calculation, we consider a nodal point I on the interface of specimen and platten. The stresses $\sigma_y(\sigma_z)$ and $\tau_{xy}(\tau_{rz})$ are obtained by the nodal forces $P(I)$ and $Q(I)$

$$\sigma_y = \frac{P(I)}{A}, \quad \tau_{xy} = \frac{Q(I)}{A} \tag{3-15}$$

which satisfy the boundary conditions (2-1) and (2-2).

In solving the problems, the shaded parts of Figs. 1 and 2 are enough to be analysed because of the symmetry of specimens and the external loads. The specimens were subdivided into triangular elements as shown in Figs. 10 and 12, for example. The calculation procedures are almost the same for both problems.

We take $t=1$ for two dimmensional problem and $\theta=1$ for axi-symmetrical problem. The calculation procedures are as follows:

i) Calculate the nodal forces $P(I)$ and $Q(I)$ on the boundary with full restraint.

ii) At the above nodal points at which $Q(I)$ is larger than $-\mu P(I)$, end restraint is released and the nodal force

$$Q(I) = -\mu P(I) \tag{3-16}$$

is replaced.

iii) Calculate the nodal forces with above condition.

iv) With these nodal forces, repeat the processes ii) and iii). If $-Q(I)/P(I)-\mu$ becomes negative, restrain the node at the position again.

v) Repeat ii)~iv) processes until sufficient convergence is observed.

In the actual calculation, at the stage i) 40 times, and at the stages ii)~iv) 5×25 times repetitions were done. The errors for Eq. (3-16) were less than 1/200,000 in all cases.

4. Results and Discussions

In the numerical calculations, Poisson's ratio was chosen as 1/6 and Eq. (3-10) or (3-13) was used to resolve the nodal forces into surface tractions. The ratios of stresses σ_y and τ_{xy} (σ_z and τ_{rz}) on the compressed end to the average stress $\sigma_{y0}(\sigma_{z0})$ for some typical examples of rectangular and cylindrical specimens are shown in Figs. 4~6 and Figs. 7~9, respectively.

Stresses in the rectangular and the cylindrical specimens with $h=1.0$ and $h=2.0$, respectively, and with the coefficients of friction $\mu=\infty$ and $\mu=0.1$ are shown in Figs. 10, 11 and 12, 13, respectively. When the ends of the specimens are fixed, some approximate solutions are available to compare with the results by the finite element method.

In the case of plane-strain and the specimen with $h=0.5$, stresses on the compressed end obtained by the finite element, finite difference[1] (mesh 20×10) and Fourier expansion[2] (up to 60 terms) methods were compared in Fig. 14. These curves show a good agreement. In axi-symmetric case Picket's solutions[3] by Fourier expansion method may be compared. The solutions by the finite element method in both cases can be considered quite reasonable for the present problems.

From the above mentioned results the following may be concluded on the influences of the end frictions on the stresses in the compressed specimens:

(i) The more the end friction is reduced, the more uniform stresses are developed in the specimen.

(ii) When the coefficients of the end frictions are approximately larger than 0.25 (for rectangular specimen), or 0.26 (for cylindrical specimen), no lubrication can be expected, that is, in these cases the stresses are the same as those of a completely restrained case.

(iii) For sufficiently small coefficients of friction to allow the end slide, shear stresses on the slided portions are cut off by $|\tau_{xy}|=\mu|\sigma_y|$ or $|\tau_{rz}|=\mu|\sigma_z|$. Thus the distribution of the shear stress along the compressed end becomes like a terrace,

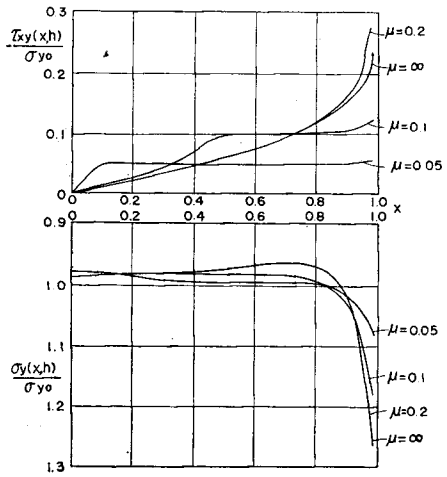

Fig. 4. Ratio of σ_y and τ_{xy} to σ_{y0} for rectangular specimen with $h=0.5$.

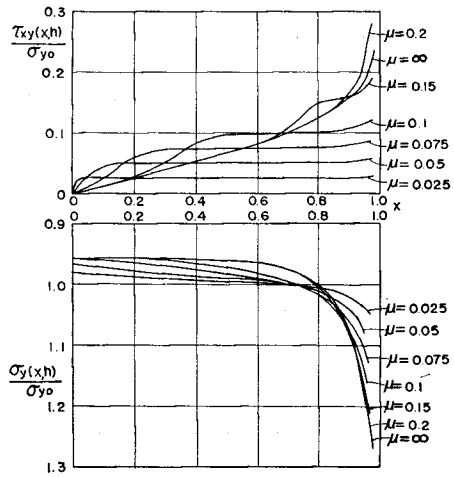

Fig. 5. Ratios of σ_y and τ_{xy} to σ_{y0} for rectangular specimen with $h=1.0$.

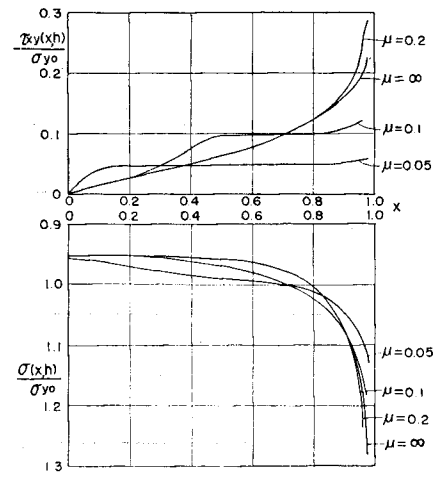

Fig. 6. Ratios of σ_y and τ_{xy} to σ_{y0} for rectangular specimen with $h=2.0$.

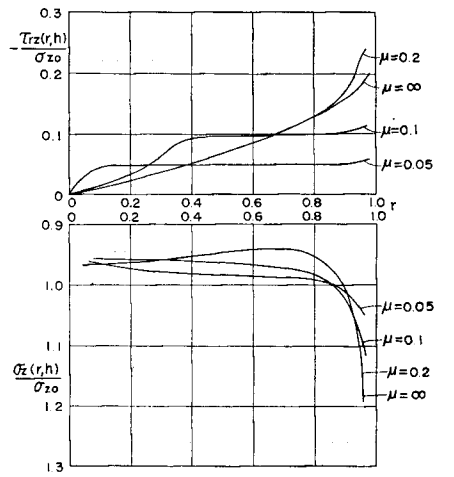

Fig. 7. Ratio of σ_z and τ_{rz} to σ_{z0} for cylindrical specimen with $h=0.5$.

as show in Figs. 6 and 9. The corners of the curves indicate the transition zone from the fixed portion to the slipped.

(iv) The deviations of the axial stress from the average are larger in cylindrical specimens than those in rectangular ones. As the end frictions are reduced, the differences are gradually decreased.

(v) The directions of the principal stress near the specimen end incline from axial direction at most 13.1 and 12.9 degrees in cylindrrical and rectangular specimens for full end restraint, respectively.

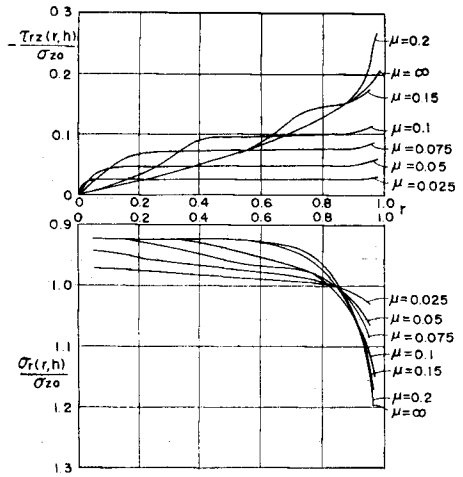

Fig. 8. Ratios of σ_z and τ_{rz} to σ_{z0} for cylindrical specimen with $h=1.0$.

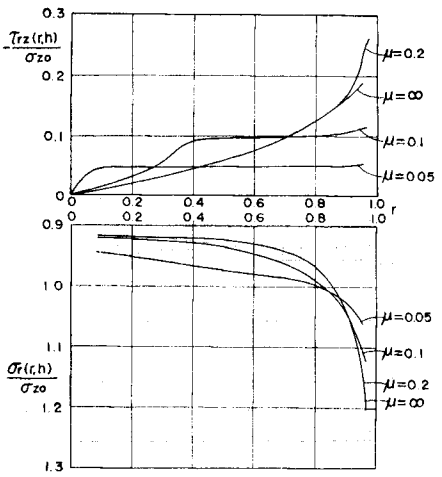

Fig. 9. Ratios of σ_z and τ_{rz} to σ_{z0} for cylindrical specimen with h=2.0.

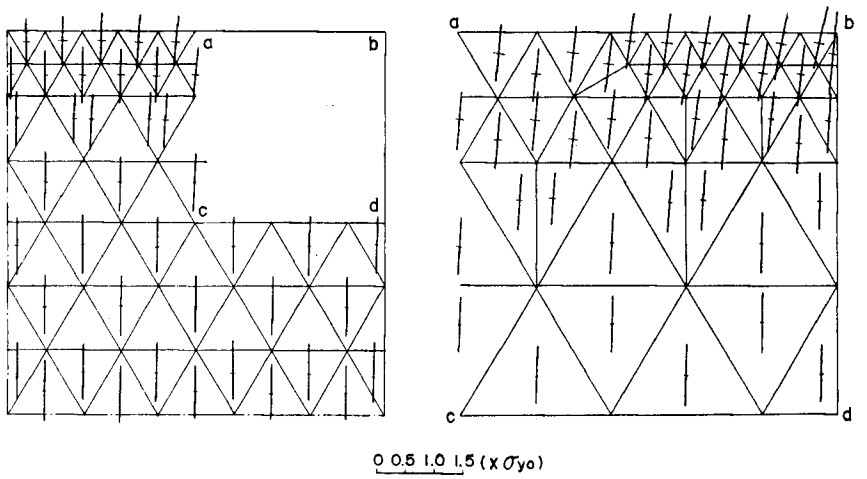

Fig. 10. Stresses in rectangular specimen with $h=1.0$ and $\mu=\infty$.

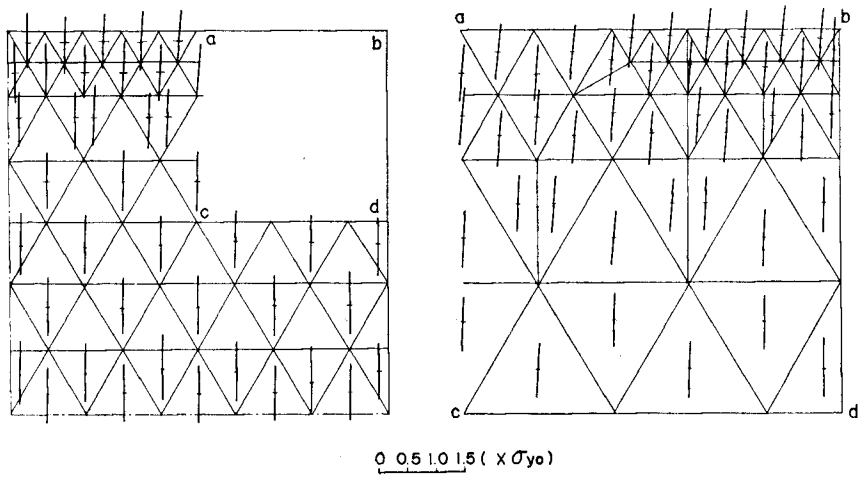

Fig. 11. Stresses in rectangular specimen with $h=1.0$ and $\mu=0.1$.

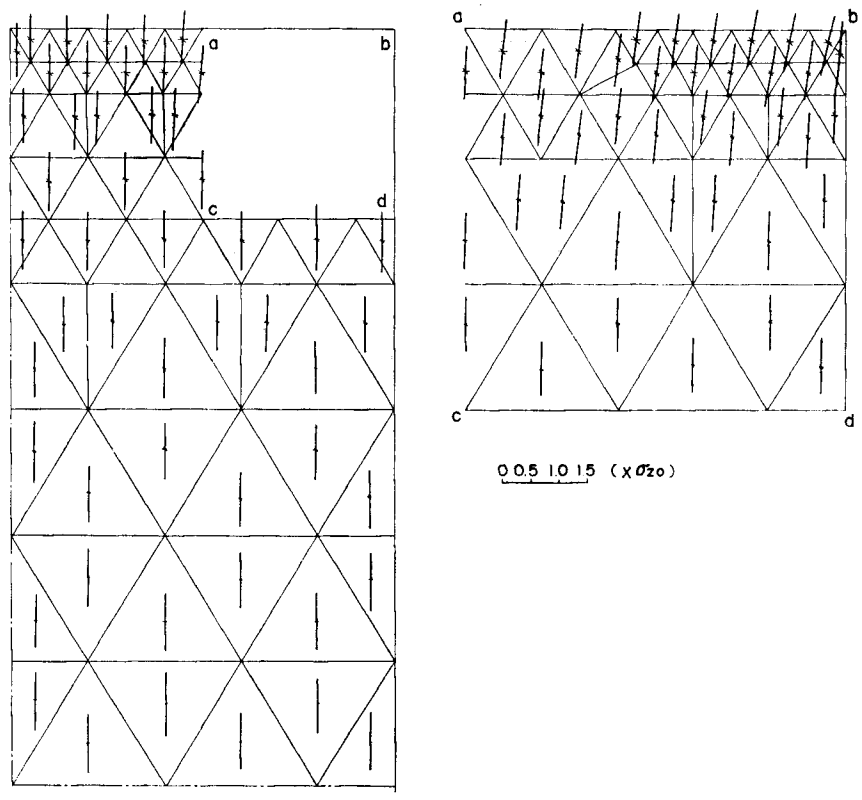

Fig. 12. Stresses in cylindrical specimen with $h=2.0$ and $\mu=\infty$.

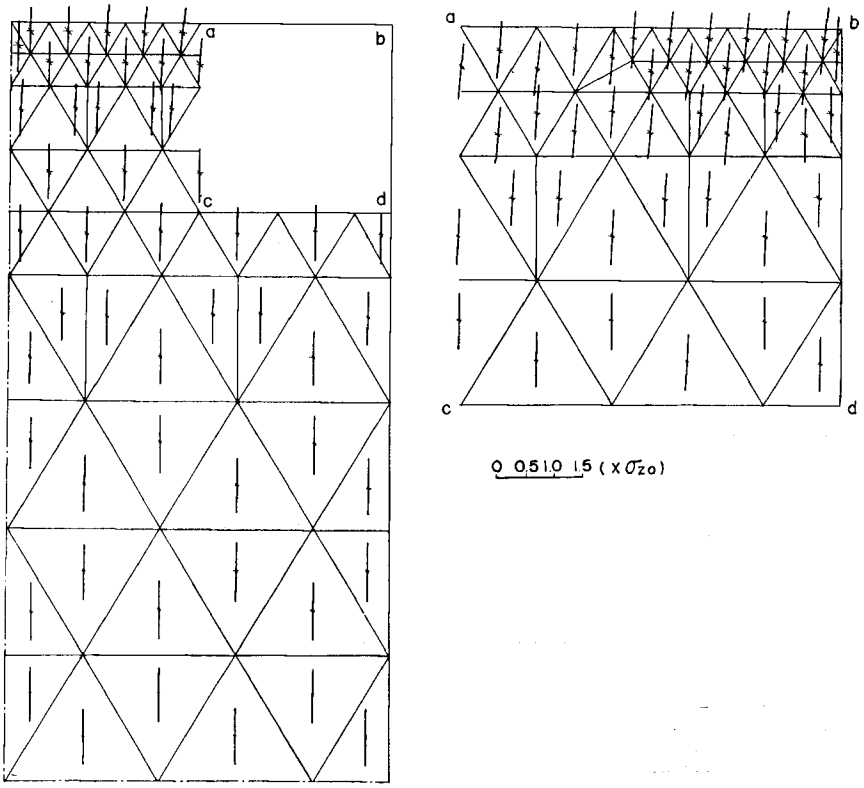

Fig. 13. Stresses in cyindrical specimen with $\mu=2.0$ and $\mu=0.1$.

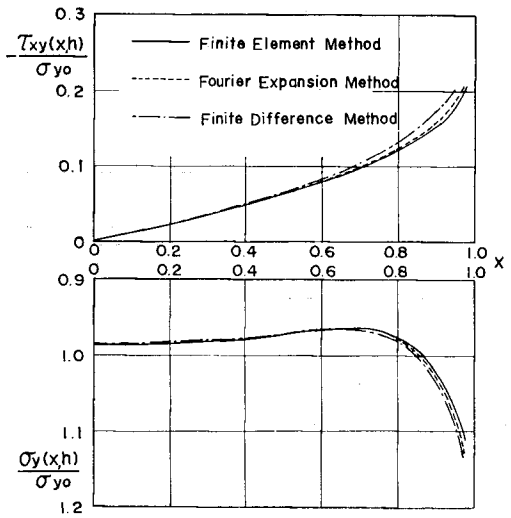

Fig 14. Comparison of boundary stresses in rectangular specimen with $h=0.5$ and $\mu=\infty$ by the use of the finite element method, Fourier expansion method and finite difference method.

(vi) Stresses in the mid-height region of the specimens are not so sensitive to the end friction as the compressed ends. Uniformity of the stress distribution of course depends on the width-height or radius-height ratios of the specimens as well as the end friction. In the cylindrical specimen with $h=2.0$, the stresses on the mid-height section are practically uniform even for the fully restrained specimens. In the short specimen with $h=1.0$, the principal stresses on the center in the mid-height section increase with coefficients of friction $\mu=\infty$, 0.1 and 0.05 about 4, 3 and 2 percent, respectively, from the average stresses.

References

1) T. Kawami; Private communication.
2) H. Kiyama; Private communication.
3) G. Pickett; J. Appl. Mech., 11, (1944).